DOI: 10.1002/ejic.200800508

Aggregation of Hexanuclear, Mixed-Valence Manganese Oxide Clusters Linked by Propionato Ligands To Form a One-Dimensional Polymer $[Mn_6O_2(O_2CEt)_{10}(H_2O)_4]_n$

Cheng-Bing Ma,[a] Ming-Qiang Hu,[a] Hui Chen,[a] Chang-Neng Chen,*[a] and Qiu-Tian Liu[a]

Keywords: Cluster-based coordination polymers / Manganese / Structural elucidation / Magnetic properties / Propionato ligands

A new discrete hexanuclear, mixed-valence Mn oxide cluster, $[Mn_6O_2(O_2CEt)_{10}(H_2O)_4]$ (**1**), has been prepared and used as the building unit for the self-assembly of a rare propionato-bridged zigzag-like chain polymer, $[Mn_6O_2(O_2CEt)_{10}(H_2O)_4]_n$ (**2**), with the retention of the Mn_6 core of **1**. Both complexes are characterized by single-crystal X-ray structure determinations and magnetic measurements. The discrete complex **1**·3H_2O crystallizes in orthorhombic space group *Pnna* with a = 14.2089(6), b = 21.4910(11), and c = 16.4247(6) Å, whereas the polymeric complex **2**·2*n*$EtCO_2H$ crystallizes in orthorhombic space group *Pbca* with a = 13.651(4), b = 25.827(8), and c = 30.312(10) Å. Variable-temperature magnetic susceptibility analyses show the presence of moderately strong antiferromagnetic interactions within the Mn_6 cluster unit in both complexes.

Introduction

As witnessed by the activity in the past few decades, there still remains considerable interest in metal–organic coordination polymers, mostly constructed from mononuclear metal centers and organic ligands, owing to their intriguing structural topologies and crystal packing motifs,[1] along with potential applications as functional materials.[2] More recently, a certain amount of attention has been paid to the use of multimetallic clusters as building units for the synthesis of such polymeric materials, primarily driven by an increasing knowledge that the metallic clusters may introduce their inherent extraordinary physical properties to the polymeric frameworks,[3] and this usually exceptional stability of polymerized products makes them more promising in applications than the metallic clusters themselves.[4]

The construction of metal–organic polymeric frameworks based on metallic cluster building blocks still remains a great challenge with regard to two interrelated aspects: the judicious choice of both the cluster building blocks that are stable enough to resist decomposition during the polymerization reaction and the linkers between the building blocks that are not only capable of retaining and/or transmitting the inherent properties of the metallic cluster to the extended system but that are also inactive towards inducing transformation of the multimetallic cluster core into the common single metal center structure. A few studies have therefore been carried out to construct such polymeric frameworks through the linking of large or intermediate-sized, multinuclear, mixed-valence manganese oxide clusters as building units,[5] although in many cases, unusual magnetic exchange interactions between oxo-bridged Mn ions allow the Mn_xO_y-containing clusters to be attractive candidates for the design of magnetic functional materials.[6]

The magnetic properties of hexanuclear clusters of the type $[Mn_6O_2(RCO_2)_{10}L_4]$, which exhibit spin frustration, have well been documented.[6,7] Replacement of the neutral capping ligand L by an *exo*-bidentate 4,4′-bipyridine (bpy) and a nitronyl nitroxide (NIT-Me) has afforded polymeric complexes $[Mn_6O_2(t\text{BuCO}_2)_{10}(t\text{BuCO}_2\text{H})_2(\text{bpy})]_n$[5c] and $[Mn_6O_2\text{piv}_{10}(\text{thf})_{2/0}(\text{NIT-Me})_{1/2}]_n$ (piv = trimethyl acetate),[5d] respectively. The use of bpy with a long backbone is not expected to transmit intercluster exchange interactions, but was used for its linking ability,[5c] and the isolation of the heterospin NIT-Me complexes was dependent on the solvent used in the synthesis.[5d] These Mn_6 clusters therefore could be potential candidate building blocks for polymeric materials with desired magnetic properties if suitable synthetic means could be developed to link them together.

Herein, we report a new propionato-bridged, zigzag-like chain polymer, $[Mn_6O_2(O_2CEt)_{10}(H_2O)_4]_n$ (**2**), assembled from newly prepared mixed-valence Mn_6 oxide cluster

[a] State Key Laboratory of Structural Chemistry, Fujian Institute of Research on the Structure of Matter, Chinese Academy of Sciences,
Fuzhou, Fujian 350002, P. R. China
Fax: +86-591-83792395
E-mail: ccn@fjirsm.ac.cn

Supporting information for this article is available on the WWW under http://www.eurjic.org or from the author.

building units $[Mn_6O_2(O_2CEt)_{10}(H_2O)_4]$ (**1**), which undergo solvothermal treatment (Scheme 1). The discrete Mn_6 cluster **1** has a usual cagelike core, but with four water molecules ligated peripherally, while the repeating unit in polymeric complex **2** not only features a similar Mn_6 core as in **1**, but also retains the peripheral ligation of four water molecules, which differs from the above-mentioned Mn_6-based polymers $[Mn_6O_2(t\text{BuCO}_2)_{10}(t\text{BuCO}_2\text{H})_2(\text{bpy})]_n$[5c] and $[Mn_6O_2\text{piv}_{10}(\text{thf})_{2/0}(\text{NIT-Me})_{1/2}]_n$.[5d] In addition, complex **2** displays a similar magnetic behavior to that of **1**, although the separation between adjacent Mn_6 units coordinatively linked by the propionato bridge is greatly shortened relative to that found in $[Mn_6O_2(t\text{BuCO}_2)_{10}(t\text{BuCO}_2\text{H})_2(\text{bpy})]_n$.[5c]

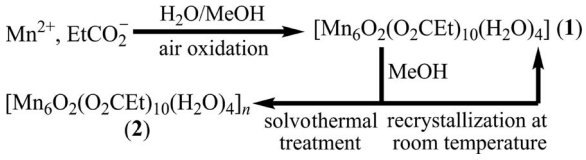

Scheme 1. Preparation of **1** and its thermally induced conversion into **2**.

Results and Discussion

Syntheses and IR Spectra

The reaction between the Mn^{2+} salt and the deprotonated propionic acid in MeOH/H_2O mixed solution gave the mixed-valent (four Mn^{II} ions and two Mn^{III} ions) complex $[Mn_6O_2(O_2CEt)_{10}(H_2O)_4]$ (**1**), which is crystallographically identified as **1**·3H_2O. It is clear that the Mn^{III} ions are formed by oxidation in air while stirring, as observed by the color change from pale yellow to black–red. The presence of the basic NaOMe reagent further promotes the oxidation process, as is almost always the case in Mn cluster chemistry. The relative stability of the Mn_6 aggregate is manifested by recrystallization as the original structure in MeOH. The stable Mn_6 aggregates are coordinatively linked into the one-dimensional polymer $[Mn_6O_2(O_2CEt)_{10}(H_2O)_4]_n$ (**2**) after solvothermal treatment. However, the brown compound **1**·3H_2O decomposes into an unknown Mn^{2+}-containing species when heated under open, reflux conditions, as observed by the occurrence of pale yellow, turbid materials. This indicates that moderate heating under sealed, autogenous pressure, and air-limiting and solvothermal conditions affords a suitable environment for polymerization of the discrete Mn_6 clusters. Little work was carried out previously that employed solvo(hydro)thermal methods for the preparation of polymeric solids based on mixed-valence Mn_x oxide clusters, owing to the known instability of these Mn clusters and proclivity to collapse when being heated. The isolation of **2**·2*n*$EtCO_2H$, however, suggests that the solvo(hydro)thermal treatment could also be developed to prepare Mn_x oxide cluster-based coordination polymers, provided that suitable strategies are adopted and suitable Mn_x oxide clusters are selected.

Both complexes exhibit almost identical IR spectra, with the exception that an additional, characteristic absorption occurs at ca. 1716 cm^{-1} in the IR spectrum of **2**·2*n*$EtCO_2H$, which is assigned to the stretching vibration of the protonated carboxyl group (COOH) of uncoordinated propionic acid. On the basis of the results from the X-ray diffraction analysis, all the propionic acid in **1**·3H_2O is deprotonated. The strong characteristic peaks at ca. 1571 cm^{-1} in both spectra are attributed to the ν_{as}(COO) mode of all the carboxylate groups, while the peaks at ca. 1468 and 1422 cm^{-1} may tentatively be assigned to the ν_s(COO) mode of certain carboxylate groups (the bidentate and the tridentate, vide infra). The medium broad bands at ca. 3430 cm^{-1} (3432 cm^{-1} for **1**·3H_2O and 3427 cm^{-1} for **2**·2*n*$EtCO_2H$) in the IR spectra of both complexes are characteristic of the H–O–H stretching vibration of the water molecules, in accordance with that of the known structure.

Description of Structures for 1·3H_2O and 2·2*n*$EtCO_2H$

Single-crystal X-ray diffraction analysis reveals that **1**·3H_2O contains one neutral discrete hexamanganese cluster **1** and three solvate water molecules in each independent crystallographic unit. The hexamanganese cluster **1** is located on a twofold axis of symmetry, which passes through the midpoint of O1–O1A along the crystallographic *a* axis, and hence half of cluster **1** is crystallographically independent. As shown in Figure 1, the cagelike $[Mn_6O_2]$ core can be described as being constructed of two edge-sharing [Mn2···Mn2A, 2.808(8) Å] Mn_4O tetrahedra, i.e. (Mn2, Mn2A, Mn3, Mn1A, O1A) and (Mn2, Mn2A, Mn3A, Mn1, O1). The peripheral ligation is accomplished by ten bridging propionato ligands (four each bridge three Mn ions in the less common 1,1,3-bridging mode and the other six each bridge two Mn ions in the common 3,3-bridging mode) and four terminal water molecules, which completes the distorted octahedral geometry around each of the Mn centers (Table 1). Bond valence sum (BVS) calculations[8] (Table S1) establish that the central Mn atoms are in the +3 oxidation state and that the other four Mn atoms in an oxidation state of +2. The two Mn^{III} atoms (Mn2 and Mn2A) exhibit Jahn–Teller (JT) distortion that is expected for high-spin Mn^{III} (d^4) in a near octahedral geometry, which is shown by axial elongation of the bonds with the μ_2-oxygen atoms (O5 and O8, and O5A and O8A) of the 1,1,3-bridging propionato ligands occupying axial positions [Mn–O = 2.217(2) and 2.235(2) Å].

The adjacent clusters are strongly associated through intercluster hydrogen bonding between the coordinated water molecules and the carboxylate oxygen atoms of adjacent clusters (Table 2) to form an interesting flat layer of a 4-connected topology with the Mn_6 units as nodes, as illustrated in Figure 2. The O···O distances of these hydrogen bonds are within the range 2.792(2)–2.880(2) Å. These hydrogen-bonded layers array parallel to each other to afford an overall multilayer stacking 3D supramolecular frame-

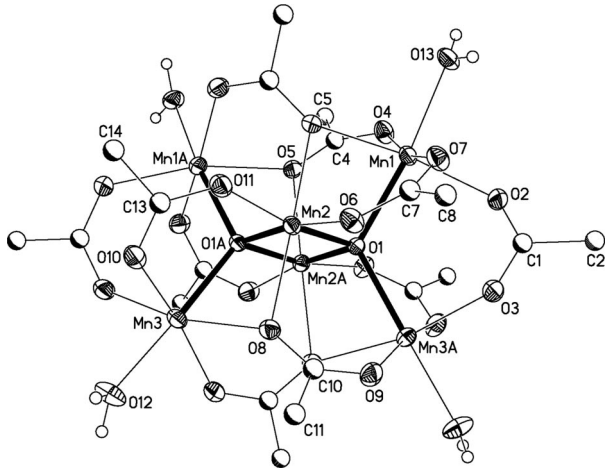

Figure 1. The structural view of **1** showing the selected atom labeling scheme (ellipsoids at 30% probability, symmetry operation: A: $x, -y + 3/2, -z + 1/2$); both methyl groups of the propionato ligands and hydrogen atoms, with the exception of those of the coordinated water molecules, are omitted for clarity.

Table 1. Selected bond lengths [Å] and angles [°] for **1**·3H_2O.

Bond lengths			
Mn1–O4	2.149(2)	Mn2–O5A	2.217(2)
Mn1–O2	2.150(2)	Mn2–O8	2.235(2)
Mn1–O7	2.174(2)	Mn3–O9A	2.146(2)
Mn1–O13	2.191(2)	Mn3–O3A	2.156(3)
Mn1–O1	2.2039(19)	Mn3–O10	2.163(3)
Mn1–O5A[a]	2.246(2)	Mn3–O1A	2.1887(18)
Mn2–O1A	1.8867(19)	Mn3–O12	2.203(3)
Mn2–O1	1.8967(19)	Mn3–O8	2.297(2)
Mn2–O6	1.943(2)	Mn2···Mn2A	2.8080(8)
Mn2–O11	1.966(2)		
Bond angles			
O4–Mn1–O2	101.12(10)	O6–Mn2–O5A	92.75(9)
O4–Mn1–O7	167.32(10)	O11–Mn2–O5A	84.40(9)
O2–Mn1–O7	83.25(10)	O1A–Mn2–O8	86.07(8)
O4–Mn1–O13	86.96(10)	O1–Mn2–O8	97.52(8)
O2–Mn1–O13	93.90(10)	O6–Mn2–O8	85.35(9)
O7–Mn1–O13	80.84(10)	O11–Mn2–O8	92.83(9)
O4–Mn1–O1	98.83(8)	O5A–Mn2–O8	176.71(8)
O2–Mn1–O1	94.23(8)	O9A–Mn3–O3A	97.42(10)
O7–Mn1–O1	92.66(8)	O9A–Mn3–O10	166.74(11)
O13–Mn1–O1	168.92(9)	O3A–Mn3–O10	90.52(11)
O4–Mn1–O5A	91.80(9)	O9A–Mn3–O1A	96.95(8)
O2–Mn1–O5A	165.83(9)	O3A–Mn3–O1A	90.21(8)
O7–Mn1–O5A	85.34(9)	O10–Mn3–O1A	93.62(8)
O13–Mn1–O5A	92.55(9)	O9A–Mn3–O12	87.69(11)
O1–Mn1–O5A	77.90(7)	O3A–Mn3–O12	90.52(11)
O1A–Mn2–O1	84.16(9)	O10–Mn3–O12	81.61(11)
O1A–Mn2–O6	171.31(9)	O1A–Mn3–O12	175.18(10)
O1–Mn2–O6	95.60(10)	O9A–Mn3–O8	87.75(9)
O1A–Mn2–O11	94.45(9)	O3A–Mn3–O8	167.65(9)
O1–Mn2–O11	169.43(9)	O10–Mn3–O8	86.63(9)
O6–Mn2–O11	87.35(11)	O1A–Mn3–O8	78.00(7)
O1A–Mn2–O5A	95.89(8)	O12–Mn3–O8	100.93(11)
O1–Mn2–O5A	85.32(8)		

[a] Symmetry code: A: $x, -y + 3/2, -z + 1/2$.

work in which the adjacent layers interact through possible intermolecular hydrogen-bonding interactions involving the uncoordinated water molecules (Figure S1).

Table 2. Hydrogen-bonding parameters [lengths Å, angles °] in **1**·3H_2O and **2**·2*n*$EtCO_2H$.[a]

D–H···A	*d*(D–H)	*d*(H···A)	∠DHA	*d*(D···A)
1·3H_2O				
O12–H12D···O14	0.828	2.012	139.63	2.697
O12–H12E···O2#1	0.849	2.051	165.14	2.880
O13–H13A···O3#2	0.830	2.014	155.88	2.792
O13–H13B···O9#2	0.824	2.207	136.33	2.860
2·2*n*$EtCO_2H$				
O3–H3B···O22#3	0.836	2.119	172.71	2.951
O4–H4A···O16#4	0.858	1.906	171.56	2.758
O5–H5A···O20#5	0.839	2.040	148.44	2.790
O5–H5B···O15#5	0.839	2.068	145.70	2.802
O6–H6A···O13#6	0.839	1.916	168.92	2.743
O3–H3A···O25	0.824	1.979	171.63	2.798
O6–H6B···O28	0.825	2.121	141.69	2.816
O27–H27A···O8	0.820	1.878	175.77	2.696
O4–H4B···O29#4	0.855	1.877	174.89	2.730
O30–H30A···O12#5	0.820	1.911	175.48	2.730

[a] Symmetry codes: #1: $x - 1/2, -y + 3/2, z - 1/2$; #2: $x + 1/2, y, -z + 1$; #3: $x - 1/2, -y + 1/2, -z + 1$; #4: $x - 1/2, y, -z + 1/2$; #5: $x + 1/2, y, -z + 1/2$; #6: $x + 1/2, -y + 1/2, -z + 1$.

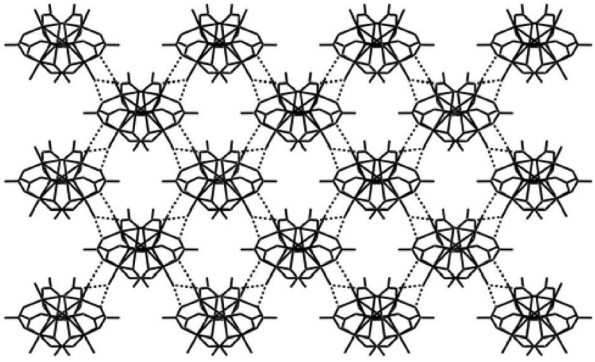

Figure 2. A view of part of the 2D 4-conneted topology layer formed by intercluster hydrogen bonds in **1**, extended along the *ac* plane; both methyl groups of the propionato ligands and all the hydrogen atoms are omitted for clarity; H-bonds are depicted as black dashed lines.

Treatment of **1**·3H_2O in methanol under solvothermal conditions affords a new 1D polymeric complex, $[Mn_6O_2(O_2CEt)_{10}(H_2O)_4]_n$·2*n*$EtCO_2H$ (**2**·2*n*$EtCO_2H$). The single-crystal X-ray diffraction analysis reveals that **2**·2*n*$EtCO_2H$ contains neutral $[Mn_6O_2(O_2CEt)_{10}(H_2O)_4]_n$ (**2**) polymers and propionic acid solvate molecules in a molar ratio of 1:2. As shown in Figure 3, the repeating unit in **2**, which resides on a crystallographic general position, possesses an almost identical cagelike structure to that of the Mn_6 cluster **1** (Table 3 and Table 4), with the exception that one propionato ligand bridges two Mn centers belonging to adjacent two Mn_6 clusters; however, such a ligand in cluster **1** fuses two intracluster Mn atoms. It is this bridging difference that results in the evolution of a completely distinct structure for polymer **2**. It is presumable that, under solvothermal conditions, one propionato bridge, at least in

a part, of the Mn_6 cluster **1** is broken first, provisionally to free one carboxylate oxygen atom and to leave one Mn center coordinatively unsaturated. As the reaction continues, the free end of the propionato ligand coordinates to the unsaturated Mn center of the adjacent cluster, thus resulting in the polymerization of the Mn_6 clusters. During the thermal treatment, partial decomposition of the Mn_6 cluster **1** occurs, with the release of some propionate ligands, as indicated by the presence of propionic acid as a solvate in **2**·2*n*$EtCO_2H$. The H protons may derive from the in situ oxidation of methanol to afford formic acid under solvothermal conditions, especially in the presence of well-known catalytic $Mn^{II/III}$ components[9] (although formic acid was not isolated from the reaction system).

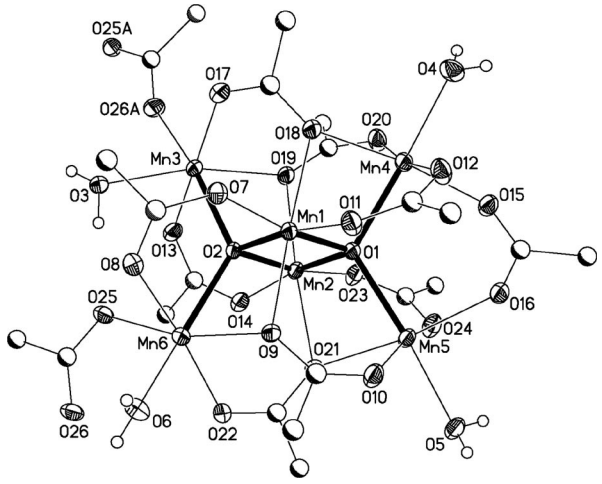

Figure 3. The structural view of a repeating unit in **2** with an adjacent propionato bridge showing the selected atom labeling scheme (ellipsoids at 30% probability, symmetry operation: A: $x - 1/2, -y + 1/2, -z + 1$); both methyl groups of the propionato ligands and hydrogen atoms, with the exception of those of the coordinated water molecules, are omitted for clarity.

Table 3. Selected bond lengths [Å] for **2**·2*n*$EtCO_2H$.

Mn1–O1	1.889(4)	Mn4–O20	2.155(5)
Mn1–O2	1.890(4)	Mn4–O4	2.184(4)
Mn1–O7	1.952(4)	Mn4–O12	2.189(5)
Mn1–O11	1.971(4)	Mn4–O1	2.189(4)
Mn1–O9	2.202(4)	Mn4–O18	2.202(4)
Mn1–O18	2.240(4)	Mn5–O10	2.130(4)
Mn2–O2	1.883(4)	Mn5–O24	2.167(5)
Mn2–O1	1.894(4)	Mn5–O1	2.180(4)
Mn2–O23	1.947(4)	Mn5–O5	2.184(4)
Mn2–O14	1.958(4)	Mn5–O16	2.186(4)
Mn2–O21	2.224(4)	Mn5–O21	2.295(4)
Mn2–O19	2.269(4)	Mn6–O25	2.140(4)
Mn3–O17	2.123(4)	Mn6–O6	2.154(4)
Mn3–O26A[a]	2.133(4)	Mn6–O22	2.189(4)
Mn3–O3	2.185(4)	Mn6–O8	2.244(4)
Mn3–O13	2.191(4)	Mn6–O9	2.249(4)
Mn3–O19	2.214(4)	Mn6–O2	2.267(4)
Mn3–O2	2.288(4)	Mn1···Mn2	2.8030(14)
Mn4–O15	2.153(4)		

[a] Symmetry code: A: $x - 1/2, -y + 1/2, -z + 1$.

Table 4. Selected bond angles [°] for **2**·2*n*$EtCO_2H$.

O1–Mn1–O2	84.17(16)	O15–Mn4–O20	92.71(18)
O1–Mn1–O7	168.83(17)	O15–Mn4–O4	90.05(19)
O2–Mn1–O7	93.01(17)	O20–Mn4–O4	86.84(18)
O1–Mn1–O11	95.46(17)	O15–Mn4–O12	87.78(18)
O2–Mn1–O11	171.92(17)	O20–Mn4–O12	171.06(18)
O7–Mn1–O11	88.84(18)	O4–Mn4–O12	84.24(18)
O1–Mn1–O9	97.50(15)	O15–Mn4–O1	93.90(16)
O2–Mn1–O9	86.75(15)	O20–Mn4–O1	97.50(16)
O7–Mn1–O9	93.12(16)	O4–Mn4–O1	173.98(17)
O11–Mn1–O9	85.30(16)	O12–Mn4–O1	91.37(16)
O1–Mn1–O18	84.39(15)	O15–Mn4–O18	171.28(16)
O2–Mn1–O18	99.44(15)	O20–Mn4–O18	92.89(16)
O7–Mn1–O18	85.42(16)	O4–Mn4–O18	96.93(17)
O11–Mn1–O18	88.54(17)	O12–Mn4–O18	87.71(17)
O9–Mn1–O18	173.69(16)	O1–Mn4–O18	78.74(14)
O2–Mn2–O1	84.24(15)	O10–Mn5–O24	165.8(2)
O2–Mn2–O23	169.40(17)	O10–Mn5–O1	97.00(15)
O1–Mn2–O23	96.24(17)	O24–Mn5–O1	92.25(16)
O2–Mn2–O14	93.91(16)	O10–Mn5–O5	87.04(17)
O1–Mn2–O14	170.23(17)	O24–Mn5–O5	82.58(18)
O23–Mn2–O14	87.35(19)	O1–Mn5–O5	172.12(17)
O2–Mn2–O21	99.81(15)	O10–Mn5–O16	105.69(18)
O1–Mn2–O21	84.94(15)	O24–Mn5–O16	83.93(18)
O23–Mn2–O21	90.78(17)	O1–Mn5–O16	95.83(15)
O14–Mn2–O21	85.93(17)	O5–Mn5–O16	89.55(17)
O2–Mn2–O19	86.02(14)	O10–Mn5–O21	87.36(16)
O1–Mn2–O19	95.22(15)	O24–Mn5–O21	84.25(17)
O23–Mn2–O19	83.39(16)	O1–Mn5–O21	77.12(13)
O14–Mn2–O19	94.22(16)	O5–Mn5–O21	96.37(16)
O21–Mn2–O19	174.15(15)	O16–Mn5–O21	165.98(16)
O17–Mn3–O26A[a]	90.41(17)	O25–Mn6–O6	101.51(17)
O17–Mn3–O3	100.17(17)	O25–Mn6–O22	99.88(17)
O26A–Mn3–O3	84.31(17)	O6–Mn6–O22	89.04(18)
O17–Mn3–O13	172.05(18)	O25–Mn6–O8	84.39(17)
O26A–Mn3–O13	83.28(17)	O6–Mn6–O8	82.06(17)
O3–Mn3–O13	84.07(17)	O22–Mn6–O8	170.77(17)
O17–Mn3–O19	92.22(16)	O25–Mn6–O9	165.61(15)
O26A–Mn3–O19	102.30(17)	O6–Mn6–O9	88.52(16)
O3–Mn3–O19	165.97(16)	O22–Mn6–O9	90.49(16)
O13–Mn3–O19	84.44(16)	O8–Mn6–O9	86.85(15)
O17–Mn3–O2	99.54(15)	O25–Mn6–O2	90.50(14)
O26A–Mn3–O2	170.00(16)	O6–Mn6–O2	160.84(16)
O3–Mn3–O2	92.96(14)	O22–Mn6–O2	103.68(15)
O13–Mn3–O2	86.88(14)	O8–Mn6–O2	84.35(14)
O19–Mn3–O2	78.40(13)	O9–Mn6–O2	77.27(13)

[a] Symmetry code: A: $x - 1/2, -y + 1/2, -z + 1$.

The two Mn^{II} atoms (Mn3 and Mn6) (Table S1) within one Mn_4O tetrahedron, with Mn3–O2–Mn6 = 129.06(15)°, connect to two adjacent clusters through the 3,3-bridging propionato ligands, which results in a one-dimensional, zigzag-like chain network (Figure 4). The closest distance between two Mn atoms belonging to two Mn_6 cluster units is 4.878(4) Å, which is significantly shorter than those formed by 4,4′-bipyridine-type linkers reported before.[5a–5c] To the best of our knowledge, this polymer represents the first example of a one-dimensional polymer constructed from manganese oxide clusters held together by relatively short carboxylate groups.

An interesting supramolecular network topology and crystal packing motif are also observed in the crystal structure of **2**·2*n*$EtCO_2H$. Neighboring polymeric chains connect to each other by five hydrogen-bonding interactions

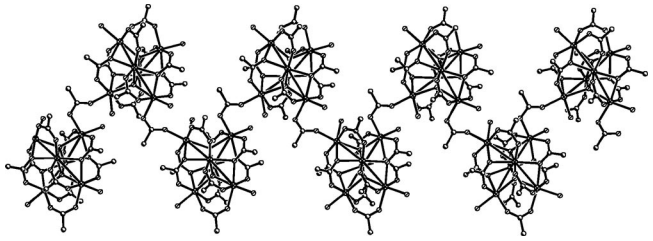

Figure 4. A view of the 1D zigzag chain of **2** extended along the *a* axis; both methyl groups of the propionato ligands and all hydrogen atoms are omitted for clarity.

(Table 2) involving four coordinated water molecules and the carboxyl O atoms (O13, O15, O16, O20, and O22) of symmetry-related chains to generate a two-dimensional, wavelike supramolecular layer with a 4-connected topology similar to that found in complex **1**. (Figure 5). These supramolecular layers are stacked parallel to each other to afford wavelike interlayer regions between which the uncoordinated propionic acid molecules are sandwiched (Figure S2).

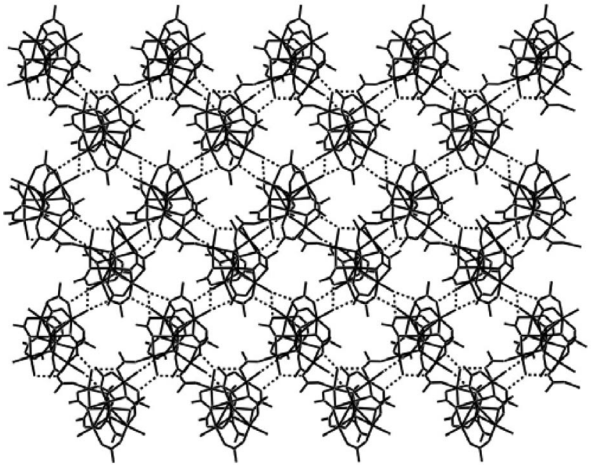

Figure 5. A view of part of 2D 4-conneted topology layer formed by interchain hydrogen bonds in **2**, extended along the *ac* plane; both methyl groups of the propionato ligands and all hydrogen atoms are omitted for clarity; H-bonds are depicted as black dashed lines.

Magnetic Properties

Variable-temperature magnetic susceptibility data were measured for both complexes in the temperature range 2.0–310 K. The resulting plots of the effective magnetic moment (μ_{eff}) and the inverse molar magnetic susceptibility ($1/\chi_M$) vs. temperature (T) for complex **1**·3H_2O are given in Figure 6 (top). At 300 K, the effective magnetic moment is 11.8 μ_B per Mn_6 unit, which is somewhat lower than the spin-only value of 13.7 μ_B expected for a set of high-spin, noninteracting $Mn^{II}_4Mn^{III}_2$ ions. The μ_{eff} value decreases gradually from room temperature down to about 70 K and then begins to decrease abruptly to reach ca. 2.5 μ_B at 2.0 K, which indicates the presence of significant intramolecular exchange interactions. The $1/\chi_M$ vs. T plot is essentially linear above 50 K and obeys the Curie–Weiss law [$\chi_M = C/(T - \theta)$] with C = 18.5 $cm^3 K^{-1}$ mol and θ = –31.6 K. The negative Weiss constant of –31.6 K indicates prevailing antiferromagnetic interactions between the manganese ions. Complex **2**·2*n*$EtCO_2H$ exhibits a similar magnetic behavior to that of complex **1**·3H_2O, as shown in Figure 6 (bottom). The least-squares fit of the data above 50 K to the Curie–Weiss equation yields the Curie constant C = 19.3 $cm^3 K^{-1}$ mol and the Weiss temperature θ = –33.2 K. The magnetic behavior displayed by these two compounds are consistent with that seen for $[Mn_6O_2(O_2CP)_{10}(py)_2(MeCN)_2]$,[6] where the prevailing antiferromagnetic exchange interaction between the two central Mn^{III} atoms within the $[Mn_6O_2]^{10+}$ core was estimated to be –42 cm^{-1}.

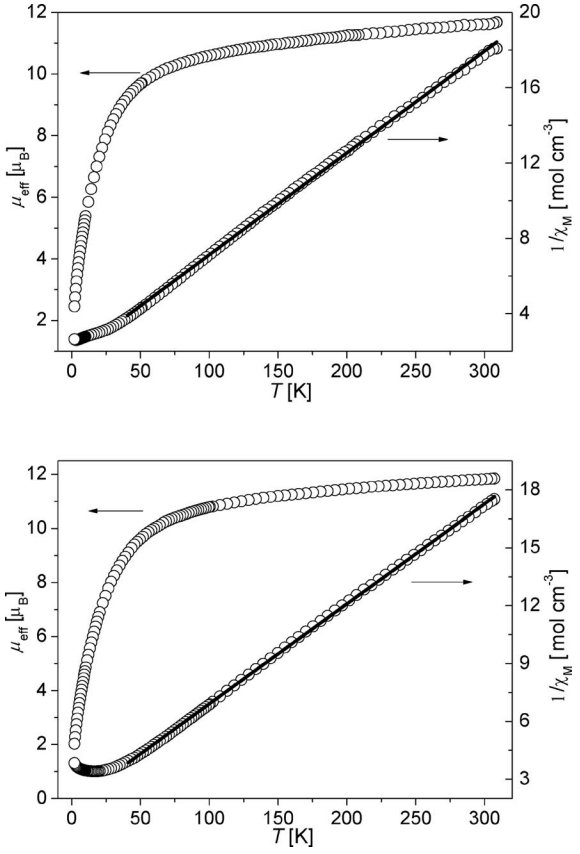

Figure 6. Plots of the observed effective magnetic moment (μ_{eff}) and the inverse molar magnetic susceptibility ($1/\chi_M$) vs. T for complexes **1**·3H_2O (top) and **2**·2*n*$EtCO_2H$ (bottom) (the solid lines represent the calculated values).

In order to detect the possible existence of a weak ferromagnetic interaction, zero-field-cooled (ZFC) and field-cooled (FC) measurements in the temperature range 2–70 K with a small applied magnetic field of 200 Oe have also been carried out on **2**·2*n*$EtCO_2H$, and the resulting plots of the temperature-dependent magnetization are shown in Figure S3. The ZFC and FC magnetization curves are almost identical, both showing a maximum for the molar susceptibility at around 16 K, which provides further evidence of antiferromagnetic interactions between the magnetic cen-

ters. These results indicate that the possibility of a weak ferromagnetic contribution within the complex can be excluded.

Conclusions

In summary, we have demonstrated a new manganese propionate zigzag-like chain coordination polymer, $[Mn_6O_2(O_2CEt)_{10}(H_2O)_4]_n$ (**2**), aggregated from newly prepared hexanuclear, mixed-valence Mn oxide cluster building units, $[Mn_6O_2(O_2CEt)_{10}(H_2O)_4]$ (**1**), with the retention of both the Mn_6 core and the four peripheral ligated water molecules of **1**. Complex **2** can be regarded as a rare example of the coordination polymer built from multinuclear, mixed-valence Mn oxide cluster units, since the relative frailness of mixed-oxidation-state Mn clusters and their inherent tendency to disproportionate make them prone to decomposition and/or other structural transformations during the polymerization process. Furthermore, the analysis of the magnetic properties reveals moderately strong antiferromagnetic interactions within the polymeric complex **2**, similar to those observed in the discrete cluster complex **1**. Thus, this study represents a preliminary successful attempt with respect to the initially intended introduction of the cluster properties to the polymeric framework. In order to advance our goal of developing new cluster-based extended systems with intriguing physical properties, it may be necessary to tune both the cluster moiety as the building unit and the bridge between the cluster units.

Experimental Section

General Remarks: All chemicals were of reagent grade and used as received. Elemental analyses were performed with a Vario EL III CHNOS element analyzer. Infrared spectra were recorded on a Magna-75 FTIR spectrophotometer by using pressed KBr pellets in the range 400–4000 cm^{-1}. Variable-temperature (2–310 K) magnetic susceptibilities were measured on a PPMS magnetometer (Quantum Design) at an applied field of 10 kG with the crystalline sample kept in the capsule for weighing. Diamagnetic corrections were estimated with Pascal's Table.

$[Mn_6O_2(O_2CEt)_{10}(H_2O)_4]\cdot 3H_2O$ ($1\cdot 3H_2O$): NaOH (30 mmol, 1.20 g) dissolved in H_2O (20 mL) was added in portions to a solution comprising $EtCO_2H$ (30 mmol, 2.3 mL) in MeOH (20 mL) over a period of 30 min. The resulting clear solution was mixed with a solution of $MnCl_2\cdot 4H_2O$ (10 mmol, 1.98 g) in MeOH (20 mL) while continuously stirring, followed by addition of solid NaOMe (5 mmol, 0.27 g). After stirring overnight, the black-red reaction mixture was filtered to remove a small amount of the brown precipitate. The filtrate was allowed to stand undisturbed at room temperature for about two months so that natural evaporation could take place, during which time a few of brown prismlike crystals of $1\cdot 3H_2O$ suitable for single-crystal X-ray diffraction were produced. A large amount of the brown–red precipitate, which was confirmed to have the same component as $1\cdot 3H_2O$ by elemental analysis, was also produced. Yield: 1.30 g (64% based on Mn). Recrystallization of the brown–red precipitate in MeOH at room temperature also afforded single crystals of $1\cdot 3H_2O$. $C_{30}H_{64}Mn_6O_{29}$ (1218.45): calcd. C 29.57, H 5.29; found C 29.66, H 5.21. IR: $\tilde{\nu}$ = 3432 (br. s), 2980 (m), 2943 (m), 1571 (vs), 1468 (m), 1424 (s), 1385 (m), 1373 (m), 1301 (m), 1246 (w), 1080 (m), 1013 (w), 889 (w), 813 (w), 613 (m), 582 (m), 469 (w) cm^{-1}.

$[Mn_6O_2(O_2CEt)_{10}(H_2O)_4]_n\cdot 2n EtCO_2H$ ($2\cdot 2nEtCO_2H$): The bulk material of $1\cdot 3H_2O$ (0.5 mmol, 0.61 g) dissolved in MeOH (15 mL) was sealed in a 20 mL Teflon-lined, stainless-steel vessel, which was then heated at 90 °C for 4 d under autogenous pressure, and then cooled to room temperature. The resulting red–brown solution was filtered, and the filtrate was allowed to stand undisturbed at room temperature for several days so that natural evaporation could take place, during which time brown, thin platelike crystals of $2\cdot 2nEtCO_2H$ suitable for single-crystal X-ray diffraction were deposited. Yield: 0.24 g (37% based on $1\cdot 3H_2O$). $C_{36}H_{70}Mn_6O_{30}$ (1312.56): calcd. C 32.94, H 5.38; found C 33.02, H 5.32. IR: $\tilde{\nu}$ = 3427 (br. s), 2983 (m), 2943 (m), 1716 (s), 1571 (vs), 1468 (s), 1421 (vs), 1373 (s), 1302 (m), 1291 (m), 1247 (w), 1217 (w), 1081 (m), 1026 (w), 888 (w), 814 (w), 666 (m), 620 (s), 577 (m), 520 (w), 470 (w) cm^{-1}.

X-ray Crystallography: Intensity data of both complexes were collected at 295(2) K on a Rigaku Mercury CCD area-detector diffractometer with graphite monochromated Mo-K_α radiation (λ = 0.71073 Å). Data reduction and cell refinement were performed with the SAINT program,[10] and absorption correction was carried out by using the SADABS program.[11] The structure was solved by direct methods and subsequent difference Fourier syntheses and refined on F^2 by full-matrix least-squares methods by using the SHELXTL-97 program package.[12] All non-hydrogen atoms were refined anisotropically. Alkyl H atoms were placed in calculated positions and treated as riding atoms, while the H atoms on both the water molecules and the protonated carboxyl groups were located from the different Fourier maps. In $1\cdot 3H_2O$, the water O14 atom was disordered over the inversion center, and the water O15 atom, located on a crystallographic general site, also displayed some disorder, so no effort was made to add H atoms to them. The methyl group carbon atoms of both one propionato ligand in $1\cdot 3H_2O$ and six propionato ligands in $2\cdot 2nEtCO_2H$ were disordered, so no action was taken to introduce H atoms to them, and the site-splitting treatments were performed on them accordingly. CCDC-687840 and CCDC-687841 contain the supplementary crystallographic data for this paper. These data can be obtained free of charge from The Cambridge Crystallographic Data Centre via www.ccdc.cam.ac.uk/data_request/cif.

Crystal Data for $1\cdot 3H_2O$: $C_{30}H_{64}Mn_6O_{29}$, Mr = 1218.45, orthorhombic, space group $Pnna$, a = 14.2089(6), b = 21.4910(11), c = 16.4247(6) Å, V = 5015.5(4) $Å^3$, Z = 4, $D_{calcd.}$ = 1.614 g/cm^{-3}, $F(000)$ = 2504, μ = 1.551 mm^{-3}, 36782 reflections collected, 5730 unique (R_{int} = 0.0316), $2\theta_{max}$ = 54.98°, GOF = 1.002, R = 0.0472 and Rw = 0.1341 [5069 observed reflections with $I > 2\sigma(I)$] for 321 parameters and 5 restraints, largest residuals $\rho_{max/min}$ = 0.449/–0.418 e $Å^{-3}$.

Crystal Data for $2\cdot 2nEtCO_2H$: $C_{36}H_{70}Mn_6O_{30}$, Mr = 1312.56, orthorhombic, space group $Pbca$, a = 13.651(4), b = 25.827(8), c = 30.312(10) Å, V = 10687(6) $Å^3$, Z = 8, $D_{calcd.}$ = 1.632 g/cm^{-3}, $F(000)$ = 5408, μ = 1.464 mm^{-3}, 64285 reflections collected, 9408 unique (R_{int} = 0.0506), $2\theta_{max}$ = 50.06°, GOF = 1.059, R = 0.0680 and Rw = 0.1987 [8199 observed reflections with $I > 2\sigma(I)$] for 650 parameters and 29 restraints, largest residuals $\rho_{max/min}$ = 0.673/–0.792 e $Å^{-3}$.

Supporting Information (see footnote on the first page of this article): Bond valence sum (BVS) calculations for each Mn ion in both complexes, two packing diagrams for the two complexes, and plots of magnetization as a function of temperature for $2\cdot 2nEtCO_2H$.

Acknowledgments

This work was supported by the National Natural Science Foundation of China (No. 20633020), the Provincial Natural Science Foundation of Fujian (No. 2008J0175), and the Fujian Province Youth Foundation (No. 2007F3112).

[1] a) O. M. Yaghi, H. Li, C. Davis, D. Richardson, T. L. Groy, *Acc. Chem. Res.* **1998**, *31*, 474–484; b) B. Moulton, M. J. Zaworotko, *Chem. Rev.* **2001**, *101*, 1629–1658; c) S. R. Batten, *CrystEngComm* **2001**, *3*, 67–73; d) L. Carlucci, G. Ciani, D. M. Proserpio, *Coord. Chem. Rev.* **2003**, *246*, 247–289; e) S. R. Batten, R. Robson, *Angew. Chem. Int. Ed.* **1998**, *37*, 1460–1494; f) M. O'Keeffe, M. Eddaoudi, H. L. Li, T. Reineke, O. M. Yaghi, *J. Solid State Chem.* **2000**, *152*, 3–20; g) M. J. Zaworotko, *Chem. Commun.* **2001**, 1–9; h) A. K. Cheetham, C. N. R. Rao, R. K. Feller, *Chem. Commun.* **2006**, 4780–4795; i) S. Surble, C. Serre, C. Mellot-Draznieks, F. Millange, G. Férey, *Chem. Commun.* **2006**, 284–286; j) T. K. Maji, R. Matsuda, S. Kitagawa, *Nat. Mater.* **2007**, *6*, 142–148; k) O. M. Yaghi, *Nat. Mater.* **2007**, *6*, 92–93; l) K. P. Rao, A. Thirumurugan, C. N. R. Rao, *Chem. Eur. J.* **2007**, *13*, 3193–3201.

[2] a) S. Kitagawa, R. Kitaura, S. Norc, *Angew. Chem. Int. Ed.* **2004**, *43*, 2334–2375; b) O. R. Evans, W. Lin, *Acc. Chem. Res.* **2002**, *35*, 511–522; c) C. Janiak, *Dalton Trans.* **2003**, 2781–2804; d) C. T. Chen, K. S. Suslick, *Coord. Chem. Rev.* **1993**, *128*, 293–322; e) J. S. Seo, D. Whang, H. Lee, S. I. Jun, J. Oh, Y. J. Jeon, K. Kim, *Nature* **2000**, *404*, 982–986; f) O. Kahn, C. Martinez, *Science* **1998**, *279*, 44–48; g) M. S. E. Fallah, E. Rentschler, A. Caneschi, R. Sessoli, D. Gatteschi, *Angew. Chem. Int. Ed. Engl.* **1996**, *35*, 1947–1948; h) M. Fujita, Y. J. Kwon, S. Washizu, K. Ogura, *J. Am. Chem. Soc.* **1994**, *116*, 1151–1152; i) S. Noro, S. Kitagawa, M. Kondo, K. Seki, *Angew. Chem. Int. Ed.* **2000**, *39*, 2081–2084; j) M. Kondo, M. Shimamura, S. Noro, S. Minakoshi, A. Asami, K. Seki, S. Kitagawa, *Chem. Mater.* **2000**, *12*, 1288–1299; k) P. M. Forster, J. Eckert, B. D. Heiken, J. B. Parise, J. W. Yoon, S. H. Jhung, J.-S. Chang, A. K. Cheetham, *J. Am. Chem. Soc.* **2006**, *128*, 16846–16850; l) A. K. Cheetham, C. N. R. Rao, *Science* **2007**, *318*, 58–59; m) G. Férey, F. Millange, M. Morcrette, C. Serre, M.-L. Doublet, J.-M. Greneche, J.-M. Tarascon, *Angew. Chem. Int. Ed.* **2007**, *46*, 3259–3263; n) P. Horcajada, C. Serre, M. Vallet-Regi, M. Sebban, F. Taulelle, G. Férey, *Angew. Chem. Int. Ed.* **2006**, *45*, 5974–5978; o) D. Tanaka, S. Kitagawa, *MRS Bull.* **2007**, *32*, 540–543; p) H. Hayashi, A. P. Cote, H. Furukawa, M. O'Keeffe, O. M. Yaghi, *Nat. Mater.* **2007**, *6*, 501–506; q) B. Chen, C. Liang, J. Yang, D. S. Contreras, Y. L. Clancy, E. B. Lobkovsky, O. M. Yaghi, S. Dai, *Angew. Chem. Int. Ed.* **2006**, *45*, 1390–1393; r) J. L. C. Rowsell, O. M. Yaghi, *Angew. Chem. Int. Ed.* **2005**, *44*, 4670–4679.

[3] a) J. J. Zhang, A. Lachgar, *J. Am. Chem. Soc.* **2007**, *129*, 250–251; b) X. M. Zhang, R. Q. Fang, H. S. Wu, *J. Am. Chem. Soc.* **2005**, *127*, 7670–7671; c) L. G. Beauvais, M. P. Shores, J. R. Long, *J. Am. Chem. Soc.* **2000**, *122*, 2763–2772; d) J. Tao, M.-L. Tong, J.-X. Shi, X.-M. Chen, *Chem. Commun.* **2000**, 2043–2044; e) J. Tao, J.-X. Shi, M.-L. Tong, X.-X. Zhang, X.-M. Chen, *Inorg. Chem.* **2001**, *40*, 6328–6330; f) W. Schmitt, E. Baissa, A. Mandel, C. E. Anson, A. K. Powell, *Angew. Chem. Int. Ed.* **2001**, *40*, 3578–3581; g) L. Carlucci, G. Ciani, D. M. Proserpio, S. Rizzato, *Chem. Commun.* **2000**, 1319–1320; h) Y. Y. Niu, Y. L. Song, H. W. How, Y. Zhu, *Inorg. Chem.* **2005**, *44*, 2553–2559; i) K. Barthelet, J. Marrot, D. Riou, G. Férey, *Angew. Chem. Int. Ed.* **2002**, *41*, 281–284; j) J. C. Dai, X. T. Wu, C. P. Cui, S. M. Hu, W. X. Du, L. M. Wu, H. H. Zhang, R. Q. Sun, *Inorg. Chem.* **2002**, *41*, 1391–1396; k) M.-L. Tong, J.-X. Shi, X.-M. Chen, *New J. Chem.* **2002**, *26*, 814–816; l) C. Livage, N. Guillou, J. Chaigneau, P. Rabu, *Mater. Res. Bull.* **2006**, *41*, 981–986; m) C.-B. Ma, C.-N. Chen, Q.-T. Liu, D.-Z. Liao, L.-C. Li, *Eur. J. Inorg. Chem.* **2008**, 1865–1870.

[4] a) H. Li, M. Eddaoudi, M. O'Keeffe, O. M. Yaghi, *Nature* **1999**, *402*, 276–279; b) J. Tao, X. Yin, Z.-B. Wei, R.-B. Huang, [1].-S. Zheng, *Eur. J. Inorg. Chem.* **2004**, 125–133.

[5] a) S. Wang, H.-L. Tsai, K. Folting, J. D. Martin, D. N. Hendrickson, G. Christou, *J. Chem. Soc., Chem. Commun.* **1994**, 671–673; b) H. J. Eppley, N. de Vries, S. Wang, S. M. Aubin, H.-L. Tsai, K. Folting, D. N. Hendriekson, G. Christou, *Inorg. Chim. Acta* **1997**, *263*, 323–340; c) K. Nakata, H. Miyasaka, K. Sugimoto, T. Ishii, K. Sugiura, M. Yamashita, *Chem. Lett.* **2002**, 658–659; d) V. Ovcharenko, E. Fursova, G. Romanenko, V. Ikorskii, *Inorg. Chem.* **2004**, *43*, 3332–3334.

[6] A. R. Schake, J. B. Vincent, Q. Li, P. D. W. Boyd, K. Folting, J. C. Huffman, D. N. Hendrickson, G. Christou, *Inorg. Chem.* **1989**, *28*, 1915–1923.

[7] a) S. Wang, H.-L. Tsai, W. E. Streib, G. Christou, D. N. Hendrickson, *J. Chem. Soc., Chem. Commun.* **1992**, 677–679; b) K. S. Gavrilenko, S. V. Punin, O. Cador, S. Golhen, L. Ouahab, V. V. Pavlishchuk, *Inorg. Chem.* **2005**, *44*, 5903–5910.

[8] a) H. H. Thorp, *Inorg. Chem.* **1992**, *31*, 1585–1588; b) I. D. Brown, D. Altermatt, *Acta Crystallogr., Sect. B* **1985**, *41*, 244–247.

[9] a) H. Wariishi, K. Valli, V. Renganathan, M. H. Gold, *J. Biol. Chem.* **1989**, *264*, 14185–14191; b) X.-M. Zhang, *Coord. Chem. Rev.* **2005**, *249*, 1201–1219.

[10] *SAINTPLUS, Data Reduction and Correction Program*, v.6.02a, Bruker AXS, Madison, WI, USA, **2000**.

[11] G. M. Sheldrick, *SADABS, Bruker/Siemens Area Detector Absorption Correction Program*, v.2.01, Bruker AXS, Madison, WI, USA, **1998**.

[12] G. M. Sheldrick, SHELXL-97, *Program for the Refinement of Crystal Structure*, University of Göttingen, Germany, **1997**.

Received: May 22, 2008
Published Online: October 16, 2008

